



Article

# The Pathogen-Induced MATE Gene *TaPIMA1* Is Required for Defense Responses to *Rhizoctonia cerealis* in Wheat

Qiang Su , Wei Rong and Zengyan Zhang \*

The National Key Facility for Crop Gene Resources and Genetic Improvement, Institute of Crop Sciences, Chinese Academy of Agricultural Sciences, Beijing 100081, China; suqiangcaas@163.com (Q.S.); 18931648844sabrina@gmail.com (W.R.)

\* Correspondence: zhangzengyan@caas.cn; Tel.: +86-10-82108781

**Abstract:** The sharp eyespot, mainly caused by the soil-borne fungus *Rhizoctonia cerealis*, is a devastating disease endangering production of wheat (*Triticum aestivum*). Multi-Antimicrobial Extrusion (MATE) family genes are widely distributed in plant species, but little is known about MATE functions in wheat disease resistance. In this study, we identified *TaPIMA1*, a pathogen-induced MATE gene in wheat, from RNA-seq data. *TaPIMA1* expression was induced by *Rhizoctonia cerealis* and was higher in sharp eyespot-resistant wheat genotypes than in susceptible wheat genotypes. Molecular biology assays showed that *TaPIMA1* belonged to the MATE family, and the expressed protein could distribute in the cytoplasm and plasma membrane. Virus-Induced Gene Silencing plus disease assessment indicated that knock-down of *TaPIMA1* impaired resistance of wheat to sharp eyespot and down-regulated the expression of defense genes (*Defensin*, *PR10*, *PR1.2*, and *Chitinase3*). Furthermore, *TaPIMA1* was rapidly induced by exogenous H<sub>2</sub>O<sub>2</sub> and jasmonate (JA) treatments, which also promoted the expression of pathogenesis-related genes. These results suggested that *TaPIMA1* might positively regulate the defense against *R. cerealis* by up-regulating the expression of defense-associated genes in H<sub>2</sub>O<sub>2</sub> and JA signal pathways. This study sheds light on the role of MATE transporter in wheat defense to *Rhizoctonia cerealis* and provides a potential gene for improving wheat resistance against sharp eyespot.

**Keywords:** wheat (*Triticum aestivum*); defense; *Rhizoctonia cerealis*; multi-antimicrobial extrusion family; *TaPIMA1*



**Citation:** Su, Q.; Rong, W.; Zhang, Z. The Pathogen-Induced MATE Gene *TaPIMA1* Is Required for Defense Responses to *Rhizoctonia cerealis* in Wheat. *Int. J. Mol. Sci.* **2022**, *23*, 3377. <https://doi.org/10.3390/ijms23063377>

Academic Editors: Josué Delgado Perón and Maria J. Andrade

Received: 13 February 2022

Accepted: 18 March 2022

Published: 21 March 2022

**Publisher's Note:** MDPI stays neutral with regard to jurisdictional claims in published maps and institutional affiliations.



**Copyright:** © 2022 by the authors. Licensee MDPI, Basel, Switzerland. This article is an open access article distributed under the terms and conditions of the Creative Commons Attribution (CC BY) license (<https://creativecommons.org/licenses/by/4.0/>).

## 1. Introduction

Common wheat (*Triticum aestivum*) is an important staple crop for global human consumption [1]. Various diseases cause great yield losses of wheat worldwide [2]. Sharp eyespot is a damaging soil-borne disease of wheat in many regions of world [3]. This disease is caused by the necrotrophic fungal pathogen *Rhizoctonia cerealis*, which mainly infects plant stems and sheaths [3,4]. China is the largest epidemic region, where at least 6.67 million hectares of wheat plants have been infected with *R. cerealis* every year since 2005 [5,6]. *R. cerealis* also infects other cereal crops (such as barley, oats, and rye), and sugar beet, cotton, and potato [3,7,8]. To date, no completely resistant wheat germplasm to *R. cerealis* has been identified, and chemical control is still limited [9]. Various studies have shown that using important resistance-associated genes would generate wheat with better resistance to sharp eyespot [5,6,9–14]. Therefore, exploration of effective resistance genes is a viable strategy to breeding wheat with resistance to sharp eyespot.

To ward off invading pathogens, plants have evolved a two-tiered innate immune system: pathogen-associated molecular pattern (PAMP)-triggered immunity (PTI), and effector-triggered immunity (ETI) [15]. By using an *Arabidopsis*–*Pseudomonas syringae* pathosystem, studies revealed that PTI and ETI are initiated by distinct activation mechanisms and involve different early signaling cascades [16,17]. Both produce reactive oxygen species

(ROS, such as  $H_2O_2$  and  $O^{2-}$ ) and induce expression of distinct or certain common defense-associated genes in the late response signals [18]. In *Arabidopsis thaliana*, previous studies showed that the up-regulated transcripts of some defense-associated genes by pathogen infection are consistent with their defensive function [19–21]. In wheat, several pathogen-induced defense-associated genes, such as *TaAGC1*, *TaRCR1*, *TaCRK3*, *TaMKK5*, *TaGATA1*, and *TaSTT3b-2B*, positively regulate the defense responses against *R. cerealis* [6,10,11,22–24]. These overexpressed genes can up-regulate the expression of downstream pathogenesis-related genes, such as *PR-1.2*, *PR2*, *chitinase3*, and *defensin* [10,11,22–28], resulting in the enhanced resistance to sharp eyespot in wheat [10,11,22–24].

Plants produce hormones, such as the salicylic acid (SA), jasmonates (JA), ethylene (ET), and abscisic acid (ABA), to amplify immune signaling and mediate defense responses against invasion of pathogens [29–31]. SA plays a positive role in resisting biotrophic and hemi-biotrophic pathogens [30,32]. JA and ET are responsible for defenses against necrotrophic pathogens and insects, while ABA is mainly involved in resisting abiotic stresses and hemi-biotrophic pathogens [30,33]. Interestingly, these hormones affect the expression of resistance/defense-associated genes to function [31–34]. For example, in wheat, *TaGATA1* responds to JA and cytokinin, and it subsequently up-regulates resistance responses to the infection of *R. cerealis* [10]. Similarly, *TaPIMP1* positively regulates defense responses to *Bipolaris sorokiniana* and drought stress through the ABA–SA signaling pathway in wheat [35]. *TaMYB29* overexpression enhances resistance to stripe rust by boosting  $H_2O_2$  accumulation, *PR* genes expression, and SA signaling in wheat [36]. Therefore, various defense-associated genes perform their functions in a highly coordinated manner through complex phytohormone signaling networks in plants.

Multi-Antimicrobial Extrusion (MATE) transporters are present in bacteria, archaea, and all eukaryotic kingdoms and are membrane efflux transporters [37]. MATE genes are widely distributed in plant genomes, and their proteins are generally comprised of 400–550 amino acid residues that encompass a 12-transmembrane segment (TMS) and MatE domain [37]. In the model plant *Arabidopsis thaliana*, MATE transporters have been shown to function in disease resistance [38–40], aluminum toxicity tolerance [41,42], detoxification of heavy metals [43,44], and the transport of secondary metabolites, e.g., anthocyanidins [45,46], flavonoids [47], and hormones [48,49]. Interestingly, MATE transporter, ENHANCED DISEASE SUSCEPTIBILITY 5 (EDS5), is involved in SA synthesis and is required for defense against the yellow strain of *Cucumber mosaic virus* [CMV(Y)] and *Pseudomonas syringae* pathogens in *Arabidopsis* [38,49–51]. Moreover, ectopic expression of *AtDTX18*, a MATE transporter controlling the extracellular accumulation of coumaroylagmatine, improves resistance of transgenic potato to *Phytophthora infestans* and *Botrytis cinerea* [40]. Conversely, *ADS1* negatively regulates *Arabidopsis* against *P. syringae* (*PstDC3000*) by down-regulating the accumulation of SA and the expression of *PR1* homolog genes [39]. Similarly, ectopic expression of *OsMATE1* and *OsMATE2* in *Arabidopsis* negatively regulates resistance to *PstDC3000* and affects plant growth and development [52]. In a previous study, RNA-seq data showed that in wheat, a MATE gene with sequence number *TraesCS2B01G296000* was upregulated and might be associated with defense to *Fusarium graminearum* [53]. However, the functional roles of MATEs in defense of *R. cerealis* remain unknown in wheat.

In this study, we identified a pathogen-induced MATE transporter named *TaPIMA1* from a set of wheat RNA-seq transcriptome data and revealed that *TaPIMA1* participated in resistance responses to *R. cerealis* in wheat. The expression of *TaPIMA1* was induced by *R. cerealis*,  $H_2O_2$ , and JA. Virus-Induced Gene Silencing (VIGS) and disease assessment results showed that *TaPIMA1* was required for wheat resistance to sharp eyespot. *TaPIMA1* positively regulated the expression profiles of at least 4 *PR* genes.

## 2. Results

### 2.1. Identification of *TaPIMA1* by Transcriptomic Analysis

To identify resistance-related genes to *R. cerealis* in wheat, we analyzed RNA-seq data of the sharp eyespot resistant and susceptible recombinant inbred lines (RILs, derived from Shanhongmai × Wenmai6) [11]. In previous studies, some MATE transporters, e.g., AtEDS5, AtADS1, OsMATE1, OsMATE2, were shown to play important roles in disease resistance responses in *Arabidopsis* and rice [38,39]. Herein, we focused on mining wheat MATE transporters that were up-regulated in the resistant RILs than in the susceptible RILs. As a result, a MATE gene with sequence number *TraesCS3B02G563500.1*, named *TaPIMA1*, showed much higher expression levels in resistant RILs (RIL-R) compared with susceptible RILs (RIL-S) (Figure 1A). Furthermore, qRT-PCR analysis showed that *TaPIMA1* expression was significantly induced by *R. cerealis* in the resistant wheat cultivars Shanhongmai and CI12633 from 1 to 10 days post-inoculation (dpi) (Figure 1B). Subsequently, we investigated the expression profiles of *TaPIMA1* in different wheat cultivars at 10 dpi with *R. cerealis*. As expected, the transcript level of *TaPIMA1* was significantly higher in the resistant cultivars (Shanhongmai and CI12633) than in susceptible cultivars (Yangmai16 and Wenmai6), and the highest expression level was detected in Shanhongmai (Figure 1B,C). Moreover, at the filling stage of CI12633 plants, *TaPIMA1* was highly expressed in roots and stems, where sharp eyespot mainly occurred (Figure 1D). Taken together, the above results suggested that *TaPIMA1* might function in defense responses to *R. cerealis* in wheat.

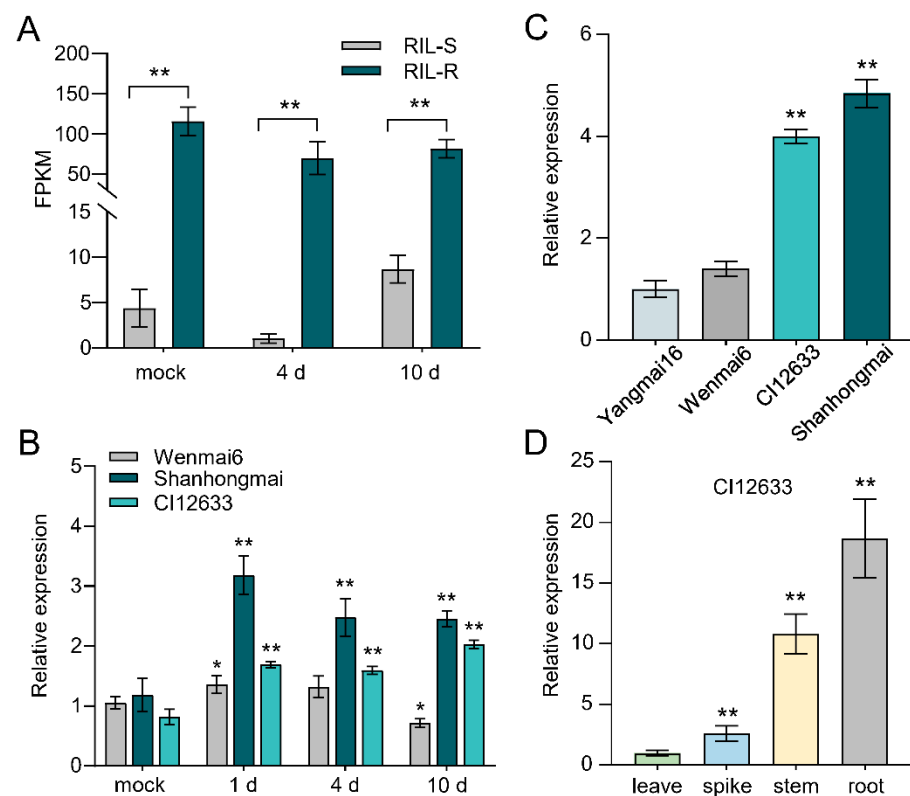


**Figure 1.** The expression profiles of *TaPIMA1* in wheat with *R. cerealis* infection. (A) The expression pattern of *TaPIMA1* in RNA-seq data of RILs. The sharp eyespot resistant/susceptible RILs were infected with *R. cerealis* and sampled at 4 and 10 dpi. (B) Transcript profiles of *TaPIMA1* in sharp eyespot-resistant cultivar CI12633 and the susceptible wheat cultivar Wenmai6 at 1, 4, and 10 dpi with *R. cerealis*. (C) The expression patterns of *TaPIMA1* in four wheat cultivars. All transcript data of *TaPIMA1* were compared with those in Yangmai16. (D) Transcriptional analyzes of *TaPIMA1* in different organs of CI12633 plants. The significant differences determined by one-way ANOVA (\*  $p < 0.05$ , \*\*  $p < 0.01$ ). Error bars indicates standard deviation.

## 2.2. Sequence and Phylogenetic Analyses of TaPIMA1

The cDNA and genomic sequences of *TaPIMA1* were cloned from wheat cultivar CI12633 and determined by Sanger sequencing. Sequence alignment showed that the cDNA sequence of *TaPIMA1* displayed 100% identity with the reference sequence *TraesCS3B02G563500.1*. In addition, the genomic sequence of *TaPIMA1* contained six introns and seven exons, which was transcribed into a 1500 bp-length coding (CD) sequence (Figure 2A). The *TaPIMA1* protein has 499 amino acid (aa) residues, and its molecular weight is predicted to be 53.50 kDa. Moreover, the *TaPIMA1* protein includes two MatE domains (no. 50–210 aa and no. 271–434 aa, respectively) and 12 transmembrane helices (TMHs, no. 445–464 aa) (Figure 2B).

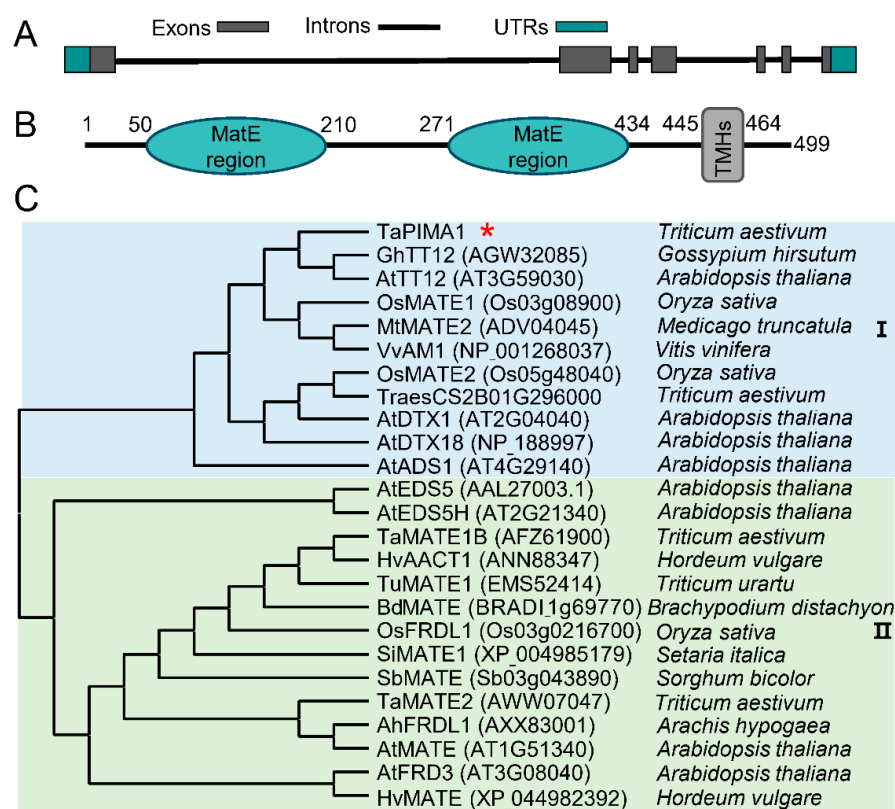


**Figure 2.** Sequence and phylogenetic analyses of *TaPIMA1*. (A) The genomic structure of *TaPIMA1* in wheat CI12633 plant. The grey frames, green frames, and lines represent exons, UTRs, and introns regions, respectively. (B) Schematic of *TaPIMA1* protein. There are two MatE domains (no. 50–210 aa and no. 271–434 aa, respectively) and a transmembrane region (12 TMHs, no. 445–464 aa) in *TaPIMA1* protein. (C) Phylogenetic analysis of the *TaPIMA1* and other MATE proteins by the maximum likelihood method. Asterisk indicates this *TaPIMA1* protein. The phylogenetic tree was constructed using MEGA 11 software. The sequences were referred to EnsemblPlants, GenBank, and Phytozome database.

The MATE family genes are functionally diverse. To determine the structural similarity of *TaPIMA1* to other MATE transporters in plants, we performed phylogenetic analysis of *TaPIMA1* and 24 other MATE proteins from wheat, rice, *Hordeum vulgare*, *Triticum urartu*, *Setaria viridis*, *Brachypodium distachyon*, *Sorghum bicolor*, *Arabidopsis*, *Arachis hypogaea*, *Gossypium hirsutum*, *Medicago truncatula*, and *Vitis vinifera* (Figure 2C, Table S1). These 24 known-function MATE proteins encompass all the reported functions of the MATE transporters, such as disease resistance [38–40,49–54], aluminum tolerance [41,42,55–60], iron translocation [56,61–63], anthocyanidin transport [47,64,65], and heavy metals detoxification [43,44,66]. As a result, the dendrogram showed that these 25 MATE proteins were mainly clustered into two clades. *TaPIMA1* and most of the defense-related MATEs,

including OsMATE1, OsMATE2, AtADS1, and TraesCS2B01G296000, were clustered into the group I (Figure 2C). TaPIMA1 was closely related to the anthocyanidins transporters *Arabidopsis* AtTT12 and *G. hirsutum* GhTT12 (Figure 2C). The full-length of TaPIMA1 shared 47.35% and 46.47% identities with GhTT12 and AtTT12, respectively (Figure S1). These preliminary analyses suggest that the MATE protein TaPIMA1 might be involved in defense and/or anthocyanidin transport.

### 2.3. Subcellular Localization of TaPIMA1 Protein

To investigate the subcellular location of TaPIMA1 in wheat, we performed the protein transient expression assay in wheat protoplasts. The *TaPIMA1* was introduced into the PH16318 construct that was driven by the 35S CaMV promoter. Then, the PH16318-TaPIMA1-GFP and PH16318-GFP (control) construct DNAs were introduced into wheat mesophyll protoplasts and expressed, respectively. Confocal microscopic observation showed that the TaPIMA1-GFP fusion protein distributed in the cytoplasm and in plasma membrane, while the control GFP was expressed throughout the cell (Figure 3). Therefore, the results suggested that TaPIMA1 localized in wheat cytoplasm and plasma membrane.

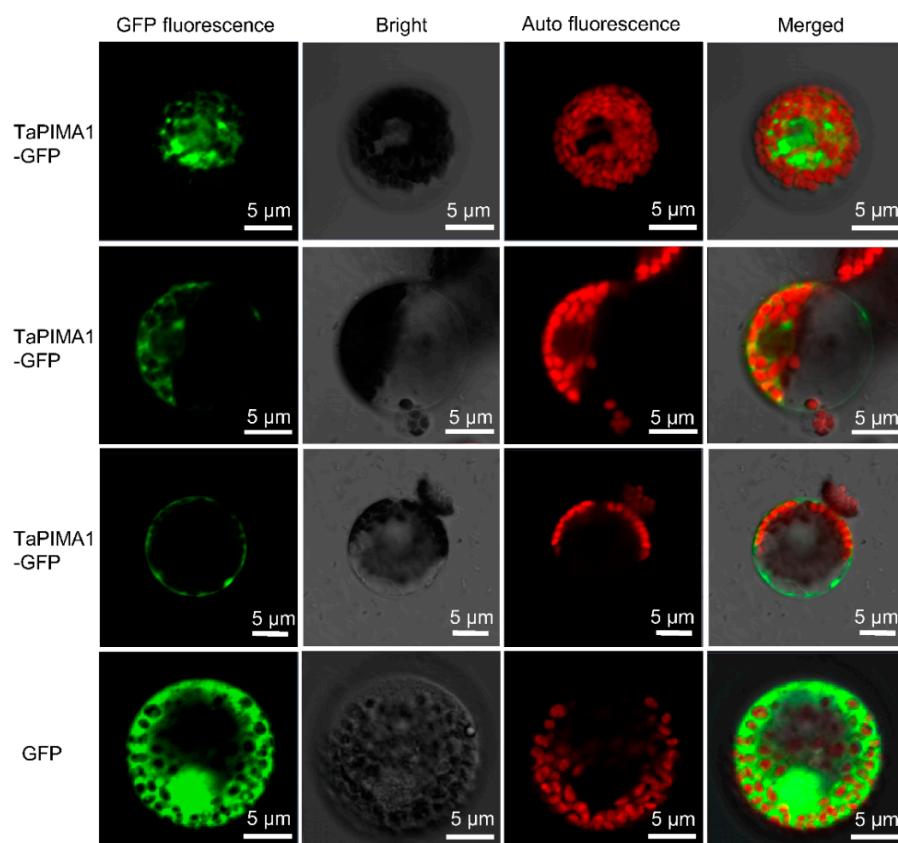


**Figure 3.** Subcellular localization of TaPIMA1 in wheat protoplasts. The GFP (control) and fused TaPIMA1-GFP were transiently expressed in wheat chloroplasts, respectively. The confocal images were taken using 488 nm wavelengths. Scale bars are each 5 µm.

### 2.4. Knock-Down of TaPIMA1 Reduced Resistance to Sharp Eyespot in Wheat

To specifically knock-down *TaPIMA1*, a 216 bp cDNA fragment specific to *TaPIMA1* was sub-cloned in an antisense orientation into the multi-clone site of the  $\gamma$  chain of *Barley stripe mosaic virus* (BSMV), generating the recombinant  $\gamma$ -*TaPIMA1* (Figure S2A,B). The BSMV  $\alpha$ ,  $\beta$ ,  $\gamma$ -*TaPIMA1* and  $\gamma$ -GFP construct DNA was individually transcribed into RNA in vitro (Figure S2C). Subsequently, these virus RNAs (BSMV  $\alpha$ ,  $\beta$ , and  $\gamma$ -*TaPIMA1* or  $\alpha$ ,  $\beta$ , and  $\gamma$ -GFP) were mixed and inoculated into the emerged third leaves of the resistant wheat cultivar CI12633 plants to execute the BSMV-mediated VIGS (BSMV-VIGS). At

10 dpi with BSMV:TaPIMA1 and BSMV:GFP, the BSMV symptom was exhibited on the new leaves of both BSMV:GFP-infected and BSMV:TaPIMA1-infected plants (Figure 4A). Additionally, the BSMV coat protein (CP) gene was detected in BSMV-infected plants by RT-PCR (Figure 4B). Moreover, the qRT-PCR showed that the mRNA levels of *TaPIMA1* were significantly decreased in BSMV:TaPIMA1-infected CI12633 plants compared with the BSMV:GFP-infected CI12633 plants (Figure 4C). These results indicated, *TaPIMA1* was successfully knocked-down in BSMV:TaPIMA1-infected CI12633 plants.

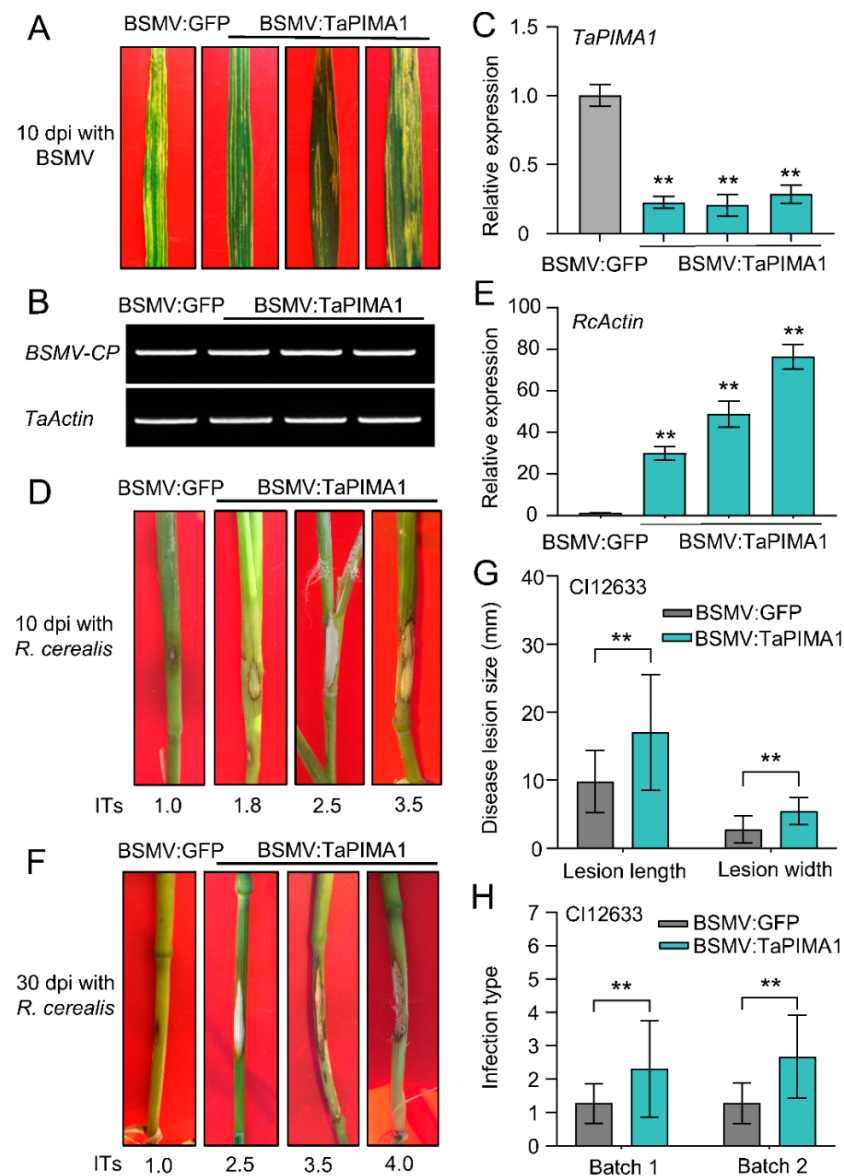


**Figure 4.** Silencing of *TaPIMA1* by BSMV-VIGS reduced resistance to *R. cerealis* in CI12633 plants. (A) The mild chlorotic mosaic symptoms were displayed on the leaves of BSMV-infected CI12633 plants at 10 dpi. (B) RT-PCR analysis of BSMV CP in the CI12633 wheat plants. The *TaActin* (TraesCS5B02G124100.1) was set as an internal control. (C) Analysis of the expression of *TaPIMA1* in BSMV-infected CI12633 plants by qRT-PCR at 10 dpi. The sharp eyespot symptoms on stems of BSMV-infected CI12633 plants at 10 (D) and 30 (F) dpi with *R. cerealis*. Disease severity was indicated by infection types (ITs). (E) qRT-PCR analysis of the biomass of *R. cerealis* in BSMV-infected CI12633 plants. (G) Disease lesion size of *R. cerealis* in *TaPIMA1*-silencing and control CI12633 plants at 30 dpi. The lesion length and width represent the lesion size of sharp eyespot. (H) The ITs of the BSMV-infected CI12633 plants in two batches. dpi, days post inoculation. The significant differences determined by one-way ANOVA (\*\*  $p < 0.01$ ). Error bars indicates standard deviation.

Next, we assessed disease severity of BSMV-infected wheat plants after inoculation with *R. cerealis*. At 10 dpi with *R. cerealis*, the sharp eyespot symptoms exhibited on the leaf sheaths and stems of BSMV-infected CI12633 plants, while the lesions of BSMV:TaPIMA1-infected plants were larger than those of control plants (Figure 4D). Furthermore, the fungal biomass, measured by the transcriptional level of *R. cerealis Actin*, was significantly higher in BSMV:TaPIMA1-infected plants (more than 29.8-fold) than that in control plants (Figure 4E). At ~30 dpi with *R. cerealis*, there were more serious lesions on the stems of BSMV-infected CI12633 plants, where the lesions were significantly larger in BSMV:TaPIMA1-infected plants compared with BSMV:GFP-infected plants (Figure 4F,G). The average necrotic length and width of BSMV:TaPIMA1-infected plants were 1.70 and 0.55 cm, whereas the BSMV:GFP-infected plants were 0.98 and 0.28 cm, respectively (Figure 4G). Two batches in functional assessments indicated that the average infection types (ITs) and disease index (DIs) of TaPIMA1-silenced CI12633 plants were 2.29 /2.67 and 45.88/53.33, while those of BSMV:GFP-infected CI12633 plants were 1.25/1.27 and 25.00/25.41, respectively (Figure 4H, Table S2). These results indicated that silencing of *TaPIMA1* significantly reduced the wheat resistance to sharp eyespot, and suggested that *TaPIMA1* is required for wheat resistance to *R. cerealis*.

### 2.5. Knock-Down of *TaPIMA1* Decreased the Expression of PR Genes

Previously studies have shown that the defense-associated even PR genes (including *PR1.2*, *PR10*, *Chitinase3*, and *defensin*) are involved in resistance responses to *R. cerealis* infection in wheat [5,22,25–27]. To investigate the regulatory pathway of *TaPIMA1* in response to *R. cerealis* infection, we examined the expression profiles of several PR genes in *TaPIMA1*-silenced CI12633 plants. As shown in Figure 5, the transcriptional levels of *PR1.2*, *PR10*, *Chitinase3*, and *defensin* were significantly downregulated in *TaPIMA1*-silenced plants compared with the control (BSMV:GFP) plants (Figure 5A–D). These results indicated that the *TaPIMA1* positively regulated the expression of PR genes, resulting in enhanced resistance to *R. cerealis*.

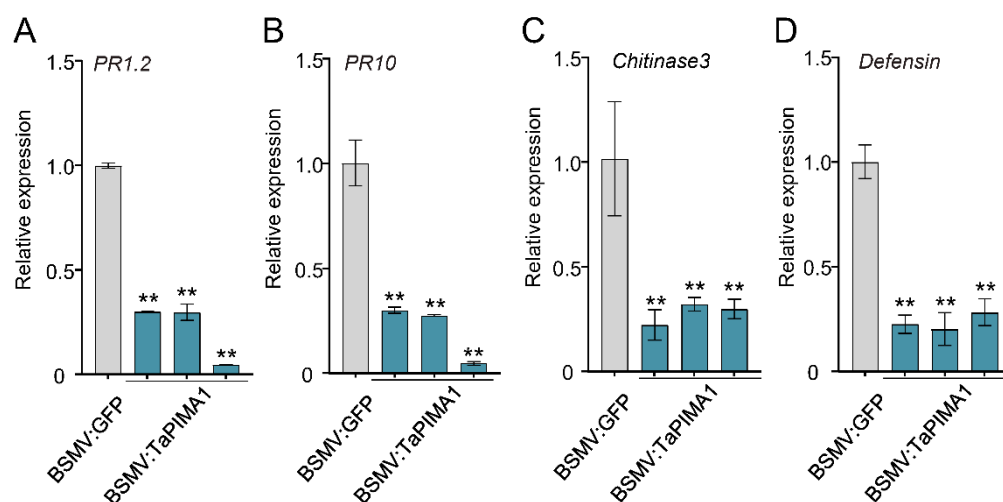


**Figure 5.** The expression levels of PR genes in *TaPIMA1*-silenced CI12633 plants at 10 dpi with *R. cerealis*. The *PR-1.2* (A, GenBank accession no. AJ007349), *PR10* (B, GenBank accession no. CA613496), *chitinase3* (C, GenBank accession no. LOC542780), and *defensin* (D, GenBank accession no. CA630387), were regulated by *TaPIMA1*. The significant differences determined by one-way ANOVA (\*\*  $p < 0.01$ ). *TaActin* was used as internal control. Error bars indicates standard deviation.

### 2.6. *TaPIMA1* and Its Regulated PR Genes Were Induced by Exogenous $H_2O_2$ and JA Stimuli

The ROS, JA and SA, play important roles in plant defense responses to pathogens [17,33,34]. Thus, we analyzed the expression profiles of *TaPIMA1* in wheat CI12633 plants treated by exogenous  $H_2O_2$ , JA, or SA. After  $H_2O_2$  treatment, the expression

level of *TaPIMA1* was dramatically elevated from 0.5 h to 12 h and peaked at 3 h (~25.64-fold over non-treatment) (Figure 6A). Upon MeJA stimulus, the transcript level of *TaPIMA1* was induced from 0.5 h to 6 h and reached a peak at 0.5 h (~2.19-fold) (Figure 6B). However, *TaPIMA1* was barely responsive to exogenous SA stimulus (Figure S3).

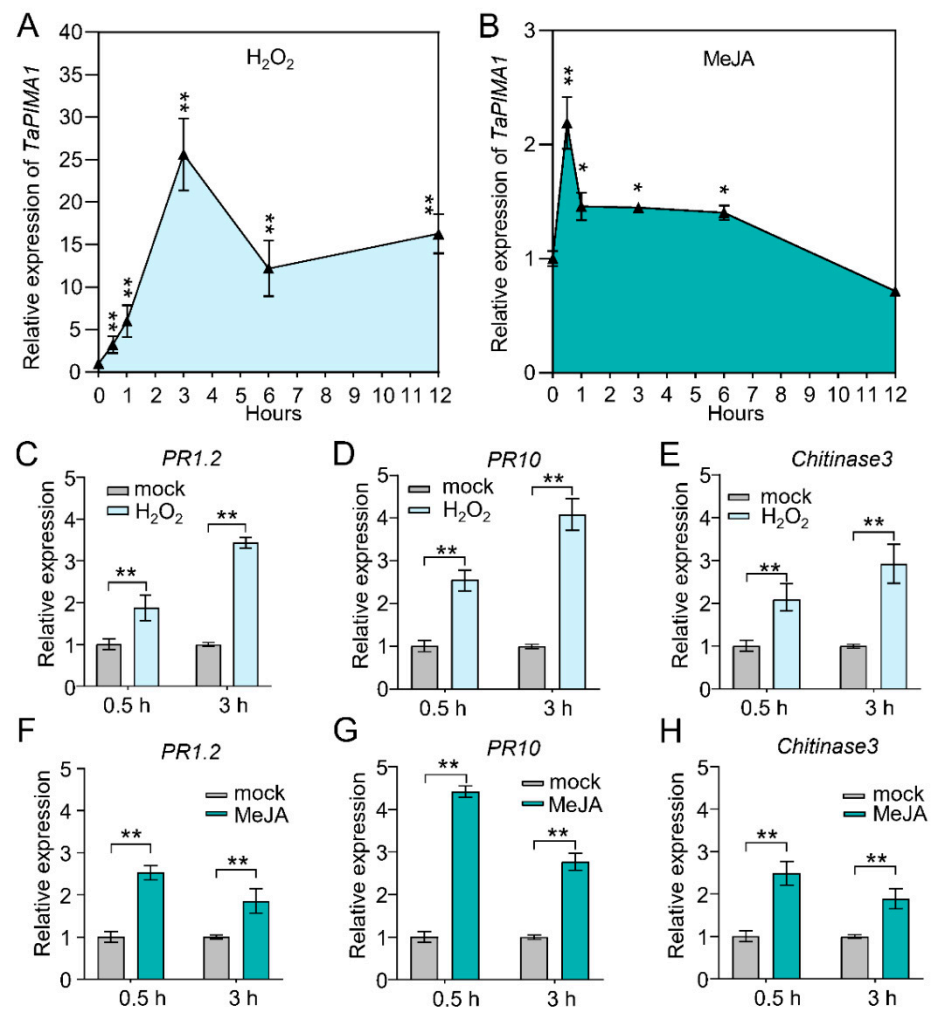


**Figure 6.** The expression profiles of *TaPIMA1* and *PR* genes in H<sub>2</sub>O<sub>2</sub>/MeJA-treated CI12633 plants. The expression profiles of *TaPIMA1* in CI12633 plants after exogenous application of H<sub>2</sub>O<sub>2</sub> (A) and MeJA (B). Expression profiles of *PR1.2*, *PR10*, and *Chitinase3* in H<sub>2</sub>O<sub>2</sub> (C–E)- and MeJA (F–H)-treated CI12633 wheat plants. The CI12633 plants were sprayed with 10 mM H<sub>2</sub>O<sub>2</sub>/0.1 mM MeJA and 0.1% Tween-20 (mock) at the four-leaf stage, respectively. The significant differences were determined by Student's *t*-test (\* *p* < 0.05, \*\* *p* < 0.01). Error bars indicate standard deviation. *TaActin* was used as internal control.

Further, the expression profiles of *PR* genes that are regulated by *TaPIMA1* were examined in CI12633 plants treated by H<sub>2</sub>O<sub>2</sub> or JA. Compared with mock-treatment, the transcription levels of *PR1.2*, *PR10*, and *Chitinase3* were significantly increased after treatment with H<sub>2</sub>O<sub>2</sub> for 0.5 h and 3 h (Figure 6C–E). Similarly, *PR1.2*, *PR10*, and *Chitinase3* were significantly up-regulated by MeJA (Figure 6F–H). These data indicated that *TaPIMA1* and its regulated *PR* genes were significantly induced by H<sub>2</sub>O<sub>2</sub> and JA.

### 3. Discussion

Wheat provides 20% of the total daily calorie expenditure of human beings in the world, but its production is threatened by sharp eyespot [5]. Developing a resistant wheat variety with disease-resistance genes is one optimal strategy to control this disease. In

this study, we provided evidence that a novel MATE gene, *TaPIMA1*, was required for resistance responses to *R. cerealis* in wheat. Here, based on the RNA-seq data and qRT-PCR analysis, we identified *TaPIMA1* that was in response to *R. cerealis*, while the expression of *TaPIMA1* was significantly higher in *R. cerealis*-resistant wheat genotypes compared with the susceptible wheat genotypes (Figure 1). Sequence analysis showed that the *TaPIMA1* deduced protein includes two MatE domains and 12 TMHs, similar to those of two rice disease-resistant transporters, OsMATE1 and OsMATE2 [52]. A phylogenetic analysis further indicated that *TaPIMA1* was classified into group I, including MATE disease-resistant transporters OsMATE1, OsMATE2 [52], AtADS1 [39], and TraesCS2B01G296000 [53], and anthocyanidins transporters *Arabidopsis* AtTT12 and *G. hirsutum* GhTT12 [46,47]. *TaPIMA1* was closely related to the anthocyanidins transporters *Arabidopsis* AtTT12 and *G. hirsutum* GhTT12. Thus, the MATE protein *TaPIMA1* might participate in the wheat defense and/or anthocyanidins transport. Generally, the MATE transporters are localized in the cytoplasm and plasma membrane to perform their transporting functions [67]. For instance, the pleiotropic anti-disease transporter EDS5 is localized in cytoplasm and exports the innate immune signal SA from chloroplast [49]. Herein, *TaPIMA1* was confirmed to localize in the wheat cytoplasm and plasma membrane (Figure 3).

In *Arabidopsis*, there are 56 MATE transporters that play important roles in plant growth, development, and resistance to biotic and abiotic stresses [37,67]. However, only a few MATE transporters with disease resistance, including resistance transporter EDS5 to viral and bacterial pathogens [38,68], *P. infestans* and *B. cinerea* resistance transporter AtDTX18 [40,69], and *P. syringae* susceptibility transporter ADS1 [39], have been characterized. The studies on functions of MATE transporters in plant immunity/defense are limited in crops, particularly in wheat. In this study, we reported that knock-down of *TaPIMA1* significantly reduced the resistance of wheat to sharp eyespot (Figure 4). Furthermore, the *TaPIMA1* transcript level was induced by *R. cerealis* and higher in root and stem tissues where sharp eyespot initially appeared; importantly, the gene transcript is higher in resistance wheat genotypes than in susceptible wheat genotypes. These data indicated that *TaPIMA1* was involved in wheat innate immunity responses to *R. cerealis*.

Some upstream immune genes substantially induce the expression of defense-related genes [23,24]. For example, heightened expression of the defense-associated genes, such as *TaSTT3b-2B*, *TaRCR1*, and *TaPIE1*, confer enhanced resistance to *R. cerealis* in transgenic wheat [6,11,23,24]. Conversely, silencing of these genes down-regulated the expression of defense genes and weakened resistance of wheat to sharp eyespot disease [10,24,36]. Herein, the transcriptional levels of *PR1.2*, *PR10*, *Defensin*, and *Chitinase3* were significantly decreased in *TaPIMA1*-silenced wheat plants, which is consistent with the performance of wheat to sharp eyespot (Figure 5). In response to ROS, plants will up-regulate defense genes, induce callose deposition, and perform hypersensitive cell death to resist pathogens [22,70]. JA and SA, acting as immune signal amplifiers, play important roles in plant responses to necrotrophic pathogens and biotrophic pathogens, respectively [29–31]. In this study, *TaPIMA1* responded rapidly to exogenous H<sub>2</sub>O<sub>2</sub> and MeJA stimuli (Figure 6A,B). Further, the expression of *TaPIMA1*-activated defense genes (*PR10*, *PR1.2*, and *Chitinase3*) was significantly up-regulated after H<sub>2</sub>O<sub>2</sub> and MeJA treatments (Figure 6C–H). In *Arabidopsis*, EDS5 contributes to the transport and accumulation of SA, while exogenous SA stimulation induces the expression of *EDS5* and enhances the resistance to biotrophic pathogens *P. syringae* [51]. Unlike EDS5, involved in the SA-mediated resistance pathway [38,49,51], *TaPIMA1* did not respond to SA but exhibited a strong inductive response to JA, similar to the MATE transporter AtDTX18 [69]. Taken together, these results suggested that H<sub>2</sub>O<sub>2</sub> and JA might participate in the *TaPIMA1*-mediated resistance to *R. cerealis* in wheat.

## 4. Materials and Methods

### 4.1. Plant and Fungus Materials, Vectors, and Primers

The resistant wheat cultivars (CI12633 and Shanhongmai) and highly susceptible wheat cultivars (Wenmai6 and Yangmai16) were used in this study. The expression profile

of *TaPIMA1* was studied in CI12633, Shanhongmai, Wenmai6, and Yangmai16. The CI12633 and Yangmai16 plants were used for BSMV-VIGS experiments. All above wheat varieties were planted in a greenhouse (14 h light/10 h dark, 15–23 °C, 90% relative humidity). The sharp eyespot pathogenic fungus *R. cerealis* strain WK207 (dominant in North China) and R0301 were used in this study.

The PH16318-GFP vector was used to express fusion protein in wheat protoplast. All BSMV vectors ( $\alpha$ ,  $\beta$ ,  $\gamma$  and  $\gamma$ -GFP) were stored in our laboratory.

The sequences of primers are listed in Table S3.

#### 4.2. Pathogen Infection and Plant Treatments

*R. cerealis* WK207 was cultured at PDA medium for 14 d. Then the *R. cerealis* WK207 was cultured with sterilized toothpicks and were covered with *R. cerealis* WK207 for 7 d at 25 °C. The leaf sheaths of wheat plants were inoculated with toothpick fragments that were covered with well-developed mycelia. The *R. cerealis* R0301 was cultured at PDA medium for 14 d and then inoculated to sterilized wheat seeds for 7 d at 25 °C. The wheat seeds carrying *R. cerealis* R0301 were inoculated into wheat roots and watered.

The CI12633 plants were grown in a greenhouse (14 h light/10 h dark, 15–23 °C, 90% relative humidity) and sprayed with 10 mM H<sub>2</sub>O<sub>2</sub> or 0.1 mM MeJA at the 4-leaf stage. At the same time, CI12633 plants were sprayed with 0.1% Tween-20 as control for all treatments. Then, the leaves were harvested at 0 h (mock), 0.5 h, 1 h, 3 h, 6 h, and 12 h after treatment.

#### 4.3. RIL Population Construction and RNA-Seq Analysis

F<sub>10</sub> RILs, derived from a cross between the sharp eyespot resistant cultivar Shanhongmai and the highly susceptible cultivar Wenmai6, were created using the single seed descent method, which were kindly provided by Professor Jizeng Jia (ICS, CAAS, China). The F<sub>11–13</sub> RILs were planted in Beijing (116°33' E, 39°96' N; 7 October–10 June) and Nanjing (118°88' E, 32°03' N; 7 November–31 May) to assess disease resistance against *R. cerealis* R0301 in 2013, 2014, and 2015. According to the assessment results, we selected three resistant RILs with DIs of 27.3, 28.69, and 30.42, and three highly susceptible RILs with DIs of 56.77, 67.19, and 64.19, in F<sub>13</sub> generation plants for RNA-seq analysis as previously described [11]. At the tillering stage, all resistant/susceptible RILs were inoculated with *R. cerealis* WK207. Leaf sheath samples of the inoculated parts were sampled at 0 d (mock), 4 d, and 10 d after inoculation with *R. cerealis*, while three biological replicates were analyzed.

Then, the RNAs of samples were used to deep RNA-Seq based on the HiSeq 2000/2500 platform (Illumina, CA, USA) supported by Biomarker Technologies (Beijing, China). All raw data in FASTQ format (raw reads) were processed using in-house Perl scripts. Clean data (clean reads) were obtained by discarding low-quality reads, reads containing adapters and ploy-N (N > 10%). Screening for differentially expressed genes between resistant and susceptible RILs that have a log<sub>2</sub> ratio greater than 1.0 (false discovery rate  $p < 0.05$ ), and the expression differences between different biological replicates were consistent [11]. The number of transcript fragments per kilobase per million mapped reads for each gene was calculated based on the length of each gene and the number of fragments mapped to that gene.

#### 4.4. Cloning and Bioinformatics Analysis of *TaPIMA1*

The full-length open reading frame (ORF) of *TaPIMA1* was amplified by nested PCR using primers pairs (TaPIMA1-FQ-F1/R1 and TaPIMA1-FQ-F2/R2) from CI12633 plants. Then, all PCR products were cloned into T vector (Takara, Tokyo, Japan) and confirmed by sequencing. The sequence of *TaPIMA1* and its homologues were referred to NCBI (<https://www.ncbi.nlm.nih.gov/> (accessed on 25 December 2021)) and Ensemble Plants database (<http://plants.ensembl.org> (accessed on 25 December 2021)). The Clustal Omega (<https://www.ebi.ac.uk/Tools/msa/clustalo/> (accessed on 25 December 2021)) web program was

used to perform the multiple sequence alignment. Additionally, MEGA 11 software was used to construct the phylogenetic tree by the maximum likelihood method.

#### 4.5. DNA and RNA Extraction, and qRT-PCR

Genomic DNA was extracted with CTAB. The leaves of wheat plants were harvested at 10 dpi and stored at  $-80^{\circ}\text{C}$ . Total RNA was extracted using TRIzol (Invitrogen, Carlsbad, CA, USA) according to the manufacturers operating manual. Then,  $\sim 1\ \mu\text{g}$  total RNA was reverse transcribed to cDNA using FastQuant RT Kit (Tiangen, Beijing, China). qRT-PCR reactions were performed on 7500 Fast Real-Time PCR Systems (Applied Biosystems, Foster City, MA, USA) using a SYBR Premix ExTaq kit (Takara, Tokyo, Japan). Additionally, each qPCR sample was run with three biological replicates and three technical replicates. The relative genes transcription levels were calculated by the  $2^{-\Delta\Delta\text{CT}}$  method [71]. All primers in this study for qRT-PCR are listed in Table S3.

#### 4.6. Subcellular Localization of *TaPIMA1*

The coding region of *TaPIMA1* without termination codon was amplified using primers *TaPIMA1*-sub-F/R and sub-cloned to the PH16318-GFP vector, named PH16318-GFP-*TaPIMA1*. The *TaPIMA1*-GFP was driven by a CaMV 35S promoter. Wheat plants were grown in pots grown in a plant growth chamber after emergence for 7 days. The seedlings were collected to produce the wheat protoplasts referring to the protocol of Liu et al. [10]. Then,  $\sim 10\ \mu\text{g}$  plasmid DNA of PH16318-GFP (control) and PH16318-GFP-*TaPIMA1* were introduced into wheat protoplasts and cultured for 20 h, respectively. Finally, the incubated protoplasts were imaged by confocal laser scanning microscope LSM 700 (Zeiss, Jena, Germany).

#### 4.7. BSMV-VIGS in Wheat

The function of *TaPIMA1* was investigated using a BSMV-VIGS in wheat as described by Holzberg [72]. Briefly, a 216 bp fragment (no. 756–955) of *TaPIMA1* ORF was cloned from CI12633 plants and then subcloned into  $\gamma$  vector in an antisense orientation that constructed the  $\gamma$ -*TaPIMA1* vector. The RNA of  $\alpha$ ,  $\beta$ ,  $\gamma$ -*TaPIMA1* and  $\gamma$ -GFP were transcribed in vitro by RiboMA Large Scale RNA Production System-T7 kit (Promega, Madison, WI, USA) according to the method described by Zhu [6]. All transcripts were mixed with and inoculated into the wheat plants at three-leaf stage. After 10 d, the fourth leaves of inoculated seedlings were harvested to extract the total RNA.

#### 4.8. Assessment of Response in BSMV-VIGS Plants to *R. cerealis*

After 20 d infection with BSMV, the leaf sheaths of infected wheat plants were inoculated with toothpick fragments carrying *R. cerealis* WK207. To promote the infection of *R. cerealis*, the inoculated site was tied up with wet absorbent cotton that was sprayed with ddH<sub>2</sub>O every day. At 30 dpi with WK207, the infection types (ITs) and disease indexes (DIs) of CI12633 plants were evaluated as described previously [5,6]. The  $\text{DI} = \sum(d_i \times l_i) \times 100 / (L \times d_{i,\text{max}})$ . The  $d_i$ ,  $l_i$ , and  $L$  represent infection type, the number of plants, and the total numbers of plants for disease assessment, respectively.

## 5. Conclusions

We identified the MATE gene *TaPIMA1* participating in wheat defense responses to *R. cerealis*. The *TaPIMA1* transcript was induced by infection of *R. cerealis* and was higher in sharp eyespot-resistant wheat genotypes than in susceptible wheat genotypes. Functional dissection revealed that *TaPIMA1*, acting as a positive regulator, is required for resistance to sharp eyespot and for the expression of PR genes including *PR1.2*, *PR10*, *Defensin*, and *Chitinase3* in wheat. *TaPIMA1* and its regulated PR genes are in response to exogenous H<sub>2</sub>O<sub>2</sub> and JA stimuli, suggesting that H<sub>2</sub>O<sub>2</sub> and JA might participate in the *TaPIMA1*-mediated resistance to *R. cerealis* in wheat. This study provides insights into role of the wheat MATE

in plant innate immunity to necrotrophic fungal pathogens. *TaPIMA1* is a potential gene for improving resistance to sharp eyespot in wheat.

**Supplementary Materials:** The following supporting information can be downloaded at <https://www.mdpi.com/article/10.3390/ijms23063377/s1>.

**Author Contributions:** Z.Z. designed the experiments, supervised the work, and revised and edited the manuscript as well the project funding acquisition. Q.S. performed the main experiments, analyzed the data, and wrote the draft manuscript. W.R. analyzed the RNA-seq data and mined the gene. All authors have read and agreed to the published version of the manuscript.

**Funding:** This work was supported by the National “Key Sci-Tech” program of China (2016ZX08002-001-004).

**Institutional Review Board Statement:** Not applicable.

**Informed Consent Statement:** Not applicable.

**Data Availability Statement:** All generated and analyzed in this study can be found in the paper and its Supplementary Materials.

**Acknowledgments:** We are grateful to Jizeng Jia (ICS, CAAS, China) for providing the F<sub>10</sub> recombinant inbred line population. We thank Huigu Chen and Shibin Cai (Jiangsu Academy of Agricultural Science) and Jinfeng Yu (Shandong Agricultural University) for providing *R. cerealis* isolates.

**Conflicts of Interest:** The authors declare no conflict of interest.

## References

- Han, Z.; Liu, Y.; Deng, X.; Liu, D.; Liu, Y.; Hu, Y.; Yan, Y. Genome-wide identification and expression analysis of expansin gene family in common wheat (*Triticum aestivum* L.). *BMC Genom.* **2019**, *20*, 101. [[CrossRef](#)] [[PubMed](#)]
- Yang, H.; Luo, P. Changes in photosynthesis could provide important insight into the interaction between wheat and fungal pathogens. *Int. J. Mol. Sci.* **2021**, *22*, 8865. [[CrossRef](#)] [[PubMed](#)]
- Hoeven, E.; Bollen, G.J. Effect of benomyl on soil fungi associated with rye. 1. Effect on the incidence of sharp eyespot caused by *Rhizoctonia cerealis*. *Neth. J. Plant Pathol.* **1980**, *86*, 163–180. [[CrossRef](#)]
- Murray, D.; Burpee, L.L. *Ceratobasidium cereale* sp.nov., the teleomorph of *Rhizoctonia cerealis*. *Trans. Brit. Mycol. Soc.* **1984**, *82*, 170–172. [[CrossRef](#)]
- Chen, L.; Zhang, Z.Y.; Liang, H.X.; Liu, H.X.; Du, L.P.; Xu, H.J.; Xin, Z.Y. Overexpression of *TiERF1* enhances resistance to sharp eyespot in transgenic wheat. *J. Exp. Bot.* **2008**, *59*, 4195–4204. [[CrossRef](#)]
- Zhu, X.L.; Yang, K.; Wei, X.N.; Zhang, Q.F.; Rong, W.; Du, L.P.; Ye, X.G.; Qi, L.; Zhang, Z.Y. The wheat AGC kinase *TaAGC1* is a positive contributor to host resistance to the necrotrophic pathogen *Rhizoctonia cerealis*. *J. Exp. Bot.* **2015**, *66*, 6591–6603. [[CrossRef](#)]
- Hamada, M.S.; Yin, Y.N.; Chen, H.G.; Ma, Z.H. The escalating threat of *Rhizoctonia cerealis*, the causal agent of sharp eyespot in wheat. *Pest Manag. Sci.* **2011**, *67*, 1411–1419. [[CrossRef](#)]
- Tomaso-Peterson, M.; Trevathan, L.E. Characterization of *Rhizoctonia*-like fungi isolated from agronomic crops and turfgrasses in Mississippi. *Plant Dis.* **2007**, *91*, 260–265. [[CrossRef](#)]
- Wu, X.J.; Cheng, K.; Zhao, R.H.; Zang, S.J.; Bie, T.D.; Jiang, Z.N.; Wu, R.L.; Gao, D.R.; Zhang, B.Q. Quantitative trait loci responsible for sharp eyespot resistance in common wheat CI12633. *Sci. Rep.* **2017**, *7*, 11799. [[CrossRef](#)]
- Liu, X.; Zhu, X.L.; Wei, X.N.; Lu, C.G.; Shen, F.D.; Zhang, X.W.; Zhang, Z.Y. The wheat LLM-domain-containing transcription factor *TaGATA1* positively modulates host immune response to *Rhizoctonia cerealis*. *J. Exp. Bot.* **2020**, *71*, 344–355. [[CrossRef](#)]
- Guo, F.L.; Wu, T.C.; Shen, F.D.; Xu, G.B.A.; Qi, H.J.; Zhang, Z.Y. The cysteine-rich receptor-like kinase *TaCRK3* contributes to defense against *Rhizoctonia cerealis* in wheat. *J. Exp. Bot.* **2021**, *72*, 6904–6919. [[CrossRef](#)] [[PubMed](#)]
- Guo, F.; Wu, T.; Xu, G.; Qi, H.; Zhu, X.; Zhang, Z. *TaWAK2A-800*, a wall-associated kinase, participates positively in resistance to fusarium head blight and sharp eyespot in wheat. *Int. J. Mol. Sci.* **2021**, *22*, 11493. [[CrossRef](#)] [[PubMed](#)]
- Qi, H.; Zhu, X.; Guo, F.; Lv, L.; Zhang, Z. The wall-associated receptor-like kinase *TaWAK7D* is required for defense responses to *Rhizoctonia cerealis* in wheat. *Int. J. Mol. Sci.* **2021**, *22*, 5629. [[CrossRef](#)] [[PubMed](#)]
- Guo, F.; Shan, Z.; Yu, J.; Xu, G.; Zhang, Z. The cysteine-rich repeat protein *TaCRR1* participates in defense against both *Rhizoctonia cerealis* and *Bipolaris sorokiniana* in wheat. *Int. J. Mol. Sci.* **2020**, *21*, 5698. [[CrossRef](#)]
- Jones, J.D.G.; Dangl, J.L. The plant immune system. *Nature* **2006**, *444*, 323–329. [[CrossRef](#)]
- Dangl, J.L.; Jones, J.D.G. Plant pathogens and integrated defence responses to infection. *Nature* **2001**, *411*, 826–833. [[CrossRef](#)]
- Barna, B.; Fodor, J.; Pogany, M.; Kiraly, Z. Role of reactive oxygen species and antioxidants in plant disease resistance. *Pest Manag. Sci.* **2003**, *59*, 459–464. [[CrossRef](#)]
- Yuan, M.H.; Jiang, Z.Y.; Bi, G.Z.; Nomura, K.; Liu, M.H.; Wang, Y.P.; Cai, B.Y.; Zhou, J.M.; He, S.Y.; Xin, X.F. Pattern-recognition receptors are required for NLR-mediated plant immunity. *Nature* **2021**, *592*, 105–109. [[CrossRef](#)]

19. Onate-Sanchez, L.; Singh, K.B. Identification of Arabidopsis ethylene-responsive element binding factors with distinct induction kinetics after pathogen infection. *Plant Physiol.* **2002**, *128*, 1313–1322. [[CrossRef](#)]
20. Lorenzo, O.; Piqueras, R.; Sanchez-Serrano, J.J.; Solano, R. Ethylene response factor1 integrates signals from ethylene and jasmonate pathways in plant defense. *Plant Cell* **2003**, *15*, 165–178. [[CrossRef](#)]
21. McGrath, K.C.; Dombrecht, D.; Manners, J.M.; Schenk, P.M.; Edgar, C.I.; Maclean, D.J.; Scheible, W.-R.; Udvardi, M.K.; Kazan, K. Repressor- and Activator-type ethylene response factors functioning in jasmonate signaling and disease resistance identified via a genome-wide screen of *Arabidopsis* transcription factor gene expression. *Plant Physiol.* **2005**, *139*, 949–959.
22. Zhu, X.L.; Lu, C.G.; Du, L.P.; Ye, X.G.; Liu, X.; Coules, A.; Zhang, Z.Y. The wheat NB-LRR gene *TaRCR1* is required for host defence response to the necrotrophic fungal pathogen *Rhizoctonia cerealis*. *Plant Biotechnol. J.* **2017**, *15*, 674–687. [[CrossRef](#)]
23. Wang, K.; Shao, Z.; Guo, F.; Wang, K.; Zhang, Z. The mitogen-activated protein kinase kinase TaMKK5 mediates immunity via the TaMKK5-TaMPK3-TaERF3 module. *Plant Physiol.* **2021**, *187*, 2323–2337.
24. Zhu, X.; Rong, W.; Wang, K.; Guo, W.; Zhou, M.; Wu, J.; Ye, X.; Wei, X.; Zhang, Z. Overexpression of *TaSTT3b-2B* improves resistance to sharp eyespot and increases grain weight in wheat. *Plant Biotechnol. J.* **2021**. [[CrossRef](#)]
25. Molina, A.; Görlach, J.; Volrath, S.; Ryals, J. Wheat genes encoding two types of PR-1 proteins are pathogen inducible, but do not respond to activators of systemic acquired resistance. *Mol. Plant-Microbe Interact.* **1999**, *12*, 53–58. [[CrossRef](#)]
26. Wehling, P.; Linz, A.; Hackauf, B.; Roux, S.R.; Ruge, B.; Klocke, B. Leaf-rust resistance in rye (*Secale cereale* L.). 1. Genetic analysis and mapping of resistance genes *Pr1* and *Pr2*. *Theor. Appl. Genet.* **2003**, *107*, 432–438. [[CrossRef](#)]
27. MunchGarthoff, S.; Neuhaus, J.M.; Boller, T.; Kemmerling, B.; Kogel, K.H. Expression of beta-1,3-glucanase and chitinase in healthy, stem-rust-affected and elicitor-treated near-isogenic wheat lines showing *Sr5*- or *Sr24*-specified race-specific rust resistance. *Planta* **1997**, *201*, 235–244. [[CrossRef](#)]
28. Zhu, X.L.; Qi, L.; Liu, X.; Cai, S.B.; Xu, H.J.; Huang, R.F.; Li, J.R.; Wei, X.N.; Zhang, Z.Y. The wheat ethylene response factor transcription factor pathogen- induced ERF1 mediates host responses to both the necrotrophic pathogen *Rhizoctonia cerealis* and freezing stresses. *Plant Physiol.* **2014**, *164*, 1499–1514. [[CrossRef](#)]
29. Verma, V.; Ravindran, P.; Kumar, P.P. Plant hormone-mediated regulation of stress responses. *BMC Plant Biol.* **2016**, *16*, 86.
30. Zhou, J.M.; Zhang, Y.L. Plant immunity: Danger perception and signaling. *Cell* **2020**, *181*, 978–989. [[CrossRef](#)]
31. Zhong, Q.; Hu, H.; Fan, B.; Zhu, C.; Chen, Z. Biosynthesis and roles of salicylic acid in balancing stress response and growth in plants. *Int. J. Mol. Sci.* **2021**, *22*, 11672. [[CrossRef](#)]
32. Loake, G.; Grant, M. Salicylic acid in plant defence—the players and protagonists. *Curr. Opin. Plant Biol.* **2007**, *10*, 466–472. [[CrossRef](#)]
33. Uji, Y.; Kashiwara, K.; Kiyama, H.; Mochizuki, S.; Akimitsu, K.; Gomi, K. Jasmonic acid-induced VQ-Motif-Containing protein OsVQ13 influences the OsWRKY45 signaling pathway and grain size by associating with OsMPK6 in Rice. *Int. J. Mol. Sci.* **2019**, *20*, 2917. [[CrossRef](#)]
34. Zhang, Y.L.; Li, X. Salicylic acid: Biosynthesis, perception, and contributions to plant immunity. *Curr. Opin. Plant Biol.* **2019**, *50*, 29–36. [[CrossRef](#)]
35. Zhang, Z.; Liu, X.; Wang, X.; Zhou, M.; Zhou, X.; Ye, X.; Wei, X. An R2R3 MYB transcription factor in wheat, TaPIMP1, mediates host resistance to *Bipolaris sorokiniana* and drought stresses through regulation of defense- and stress-related genes. *New Phytol.* **2012**, *196*, 1155–1170. [[CrossRef](#)]
36. Zhu, X.; Li, X.; He, Q.; Guo, D.; Liu, C.; Cao, J.; Wu, Z.; Kang, Z.; Wang, X. TaMYB29: A novel R2R3-MYB transcription factor involved in wheat defense against stripe rust. *Front. Plant Sci.* **2021**, *12*, 783388. [[CrossRef](#)]
37. Kuroda, T.; Tsuchiya, T. Multidrug efflux transporters in the MATE family. *BBA-Proteins Proteom.* **2009**, *1794*, 763–768. [[CrossRef](#)]
38. Ishihara, T.; Sekine, K.T.; Hase, S.; Kanayama, Y.; Seo, S.; Ohashi, Y.; Kusano, T.; Shibata, D.; Shah, J.; Takahashi, H. Overexpression of the *Arabidopsis thaliana* *EDS5* gene enhances resistance to viruses. *Plant Biol.* **2008**, *10*, 451–461. [[CrossRef](#)]
39. Sun, X.L.; Gilroy, E.M.; Chini, A.; Nurnberg, P.L.; Hein, I.; Lacomme, C.; Birch, P.R.J.; Hussain, A.; Yun, B.W.; Loake, G.J. *ADS1* encodes a MATE-transporter that negatively regulates plant disease resistance. *New Phytol.* **2011**, *192*, 471–482. [[CrossRef](#)]
40. Dobritsch, M.; Lübken, T.; Eschen-Lippold, L.; Gorzolka, K.; Blum, E.; Matern, A.; Marillonnet, S.; Böttcher, C.; Dräger, B.; Rosahl, S. MATE transporter-dependent export of hydroxycinnamic acid amides. *Plant Cell* **2016**, *28*, 583–596. [[CrossRef](#)]
41. Liu, J.P.; Magalhaes, J.V.; Shaff, J.; Kochian, L.V. Aluminum-activated citrate and malate transporters from the MATE and ALMT families function independently to confer *Arabidopsis* aluminum tolerance. *Plant J.* **2009**, *57*, 389–399. [[CrossRef](#)]
42. Magalhaes, J.V.; Liu, J.; Guimaraes, C.T.; Lana, U.G.P.; Alves, V.M.C.; Wang, Y.H.; Schaffert, R.E.; Hoekenga, O.A.; Pinerros, M.A.; Shaff, J.E.; et al. A gene in the multidrug and toxic compound extrusion (MATE) family confers aluminum tolerance in sorghum. *Nat. Genet.* **2007**, *39*, 1156–1161. [[CrossRef](#)]
43. Li, L.G.; He, Z.Y.; Pandey, G.K.; Tsuchiya, T.; Luan, S. Functional cloning and characterization of a plant efflux carrier for multidrug and heavy metal detoxification. *J. Biol. Chem.* **2002**, *277*, 5360–5368. [[CrossRef](#)]
44. Wang, J.J.; Hou, Q.Q.; Li, P.H.; Yang, L.; Sun, X.C.; Bedito, V.A.; Wen, J.Q.; Chen, B.B.; Mysore, K.S.; Zhao, J. Diverse functions of multidrug and toxin extrusion (MATE) transporters in citric acid efflux and metal homeostasis in *Medicago truncatula*. *Plant J.* **2017**, *90*, 79–95. [[CrossRef](#)]
45. Mathews, H.; Clendennen, S.K.; Caldwell, C.G.; Liu, X.L.; Connors, K.; Matheis, N.; Schuster, D.K.; Menasco, D.J.; Wagoner, W.; Lightner, J.; et al. Activation tagging in tomato identifies a transcriptional regulator of anthocyanin biosynthesis, modification, and transport. *Plant Cell* **2003**, *15*, 1689–1703. [[CrossRef](#)]

46. Gao, J.S.; Wu, N.; Shen, Z.L.; Lv, K.; Qian, S.H.; Guo, N.; Sun, X.; Cai, Y.P.; Lin, Y. Molecular cloning, expression analysis and subcellular localization of a *Transparent Testa 12* ortholog in brown cotton (*Gossypium hirsutum* L.). *Gene* **2016**, *576*, 763–769. [[CrossRef](#)]
47. Debeaujon, I.; Peeters, A.J.M.; Leon-Kloosterziel, K.M.; Koornneef, M. The *TRANSPARENT TESTA12* gene of *Arabidopsis* encodes a multidrug secondary transporter-like protein required for flavonoid sequestration in vacuoles of the seed coat endothelium. *Plant Cell* **2001**, *13*, 853–871. [[CrossRef](#)]
48. Zhang, H.; Zhu, H.; Pan, Y.; Yu, Y.; Luan, S.; Li, L. A DTX/MATE-type transporter facilitates abscisic acid efflux and modulates ABA sensitivity and drought tolerance in *Arabidopsis*. *Mol. Plant* **2014**, *7*, 1522–1532. [[CrossRef](#)]
49. Serrano, M.; Wang, B.; Aryal, B.; Garcion, C.; Abou-Mansour, E.; Heck, S.; Geisler, M.; Mauch, F.; Nawrath, C.; Métraux, J.P. Export of salicylic acid from the chloroplast requires the multidrug and toxin extrusion-like transporter EDS5. *Plant Physiol.* **2013**, *162*, 1815–1821. [[CrossRef](#)]
50. Yamasaki, K.; Motomura, Y.; Yagi, Y.; Nomura, H.; Kikuchi, S.; Nakai, M.; Shiina, T. Chloroplast envelope localization of EDS5, an essential factor for salicylic acid biosynthesis in *Arabidopsis thaliana*. *Plant Signal Behav.* **2013**, *8*, e23603. [[CrossRef](#)]
51. Nawrath, C.; Heck, S.; Parinthewong, N.; Métraux, J.P. EDS5, an essential component of salicylic acid-dependent signaling for disease resistance in *Arabidopsis*, is a member of the MATE transporter family. *Plant Cell* **2002**, *14*, 275–286. [[CrossRef](#)]
52. Tiwari, M.; Sharma, D.; Singh, M.; Tripathi, R.D.; Trivedi, P.K. Expression of OsMATE1 and OsMATE2 alters development, stress responses and pathogen susceptibility in *Arabidopsis*. *Sci. Rep.* **2014**, *4*, 3964. [[CrossRef](#)]
53. Pan, Y.; Liu, Z.; Rocheleau, H.; Fauteux, F.; Wang, Y.; McCartney, C.; Ouellet, T. Transcriptome dynamics associated with resistance and susceptibility against fusarium head blight in four wheat genotypes. *BMC Genom.* **2018**, *19*, 642. [[CrossRef](#)]
54. Parinthewong, N.; Cottier, S.; Buchala, A.; Nawrath, C.; Métraux, J.P. Localization and expression of EDS5H a homologue of the SA transporter EDS5. *BMC Plant Biol.* **2015**, *15*, 135. [[CrossRef](#)]
55. Ribeiro, A.P.; de Souza, W.R.; Martins, P.K.; Vinecky, F.; Duarte, K.E.; Basso, M.F.; da Cunha, B.A.D.B.; Campanha, R.B.; de Oliveira, P.A.; Centeno, D.C.; et al. Overexpression of BdMATE gene improves aluminum tolerance in *Setaria viridis*. *Front. Plant Sci.* **2017**, *8*, 865. [[CrossRef](#)]
56. Qiu, W.; Wang, N.; Dai, J.; Wang, T.; Kochian, L.V.; Liu, J.; Zuo, Y. AhFRDL1-mediated citrate secretion contributes to adaptation to iron deficiency and aluminum stress in peanuts. *J. Exp. Bot.* **2019**, *70*, 2873–2886. [[CrossRef](#)]
57. Liu, J.; Luo, X.; Shaff, J.; Liang, C.; Jia, X.; Li, Z.; Magalhaes, J.; Kochian, L.V. A promoter-swap strategy between the *AtALMT* and *AtMATE* genes increased *Arabidopsis* aluminum resistance and improved carbon-use efficiency for aluminum resistance. *Plant J.* **2012**, *71*, 327–337. [[CrossRef](#)]
58. Garcia-Oliveira, A.L.; Benito, C.; Guedes-Pinto, H.; Martins-Lopes, P. Molecular cloning of *TaMATE2* homoeologues potentially related to aluminium tolerance in bread wheat (*Triticum aestivum* L.). *Plant Biol.* **2018**, *20*, 817–824. [[CrossRef](#)]
59. Melo, J.O.; Martins, L.G.C.; Barros, B.A.; Pimenta, M.R.; Lana, U.G.P.; Duarte, C.E.M.; Pastina, M.M.; Guimaraes, C.T.; Schaffert, R.E.; Kochian, L.V.; et al. Repeat variants for the SbMATE transporter protect sorghum roots from aluminum toxicity by transcriptional interplay in cis and trans. *Proc. Natl. Acad. Sci. USA* **2019**, *116*, 313–318. [[CrossRef](#)]
60. Han, C.; Zhang, P.; Ryan, P.R.; Rathjen, T.M.; Yan, Z.H.; Delhaize, E. Introgression of genes from bread wheat enhances the aluminium tolerance of durum wheat. *Theor. Appl. Genet.* **2016**, *129*, 729–739. [[CrossRef](#)]
61. Yokosho, K.; Yamaji, N.; Ueno, D.; Mitani, N.; Ma, J.F. OsFRDL1 is a citrate transporter required for efficient translocation of iron in rice. *Plant Physiol.* **2009**, *149*, 297–305. [[CrossRef](#)]
62. Pineau, C.; Loubet, S.; Lefoulon, C.; Chalies, C.; Fizames, C.; Lacombe, B.; Ferrand, M.; Loudet, O.; Berthomieu, P.; Richard, O. Natural variation at the FRD3 MATE transporter locus reveals cross-talk between Fe homeostasis and Zn tolerance in *Arabidopsis thaliana*. *PLoS Genet.* **2012**, *8*, e1003120. [[CrossRef](#)]
63. Tovkach, A.; Ryan, P.R.; Richardson, A.E.; Lewis, D.C.; Rathjen, T.M.; Ramesh, S.; Tyerman, S.D.; Delhaize, E. Transposon-mediated alteration of *TaMATE1B* expression in wheat confers constitutive citrate efflux from root apices. *Plant Physiol.* **2013**, *161*, 880–892. [[CrossRef](#)] [[PubMed](#)]
64. Zhao, J.; Huhman, D.; Shadle, G.; He, X.Z.; Sumner, L.W.; Tang, Y.; Dixon, R.A. MATE2 mediates vacuolar sequestration of flavonoid glycosides and glycoside malonates in *Medicago truncatula*. *Plant Cell* **2011**, *23*, 1536–1555. [[CrossRef](#)]
65. Gomez, C.; Terrier, N.; Torregrosa, L.; Vialet, S.; Fournier-Level, A.; Verries, C.; Souquet, J.M.; Mazauric, J.P.; Klein, M.; Cheynier, V.; et al. Grapevine MATE-type proteins act as vacuolar H<sup>+</sup>-dependent acylated anthocyanin transporters. *Plant Physiol.* **2009**, *150*, 402–415. [[CrossRef](#)]
66. Ferreira, J.R.; Faria, B.F.; Comar, M.; Delatorre, C.A.; Minella, E.; Pereira, J.F. Is a non-synonymous SNP in the *HvAACT1* coding region associated with acidic soil tolerance in barley? *Genet. Mol. Biol.* **2017**, *40*, 480–490. [[CrossRef](#)] [[PubMed](#)]
67. Devanna, B.N.; Jaswal, R.; Singh, P.K.; Kapoor, R.; Jain, P.; Kumar, G.; Sharma, Y.; Samantaray, S.; Sharma, T.R. Role of transporters in plant disease resistance. *Physiol. Plant.* **2021**, *171*, 849–867. [[CrossRef](#)] [[PubMed](#)]
68. Carviel, J.L.; Wilson, D.C.; Isaacs, M.; Carella, P.; Catana, V.; Golding, B.; Weretilnyk, E.A.; Cameron, R.K. Investigation of intercellular salicylic acid accumulation during compatible and incompatible *Arabidopsis-Pseudomonas syringae* interactions using a fast neutron-generated mutant allele of *EDS5* identified by genetic mapping and whole-genome sequencing. *PLoS ONE* **2014**, *9*, e88608. [[CrossRef](#)] [[PubMed](#)]
69. Li, J.; Meng, Y.; Zhang, K.; Li, Q.; Li, S.; Xu, B.; Georgiev, M.I.; Zhou, M. Jasmonic acid-responsive RRTF1 transcription factor controls *DTX18* gene expression in hydroxycinnamic acid amide secretion. *Plant Physiol.* **2021**, *185*, 369–384. [[CrossRef](#)] [[PubMed](#)]

70. Lehmann, S.; Serrano, M.; L'Haridon, F.; Tjamos, S.E.; Metraux, J.P. Reactive oxygen species and plant resistance to fungal pathogens. *Phytochemistry* **2015**, *112*, 54–62. [[CrossRef](#)]
71. Livak, K.J.; Schmittgen, T.D. Analysis of relative gene expression data using real-time quantitative PCR and the  $2^{-\Delta\Delta CT}$  method. *Methods* **2001**, *25*, 402–408. [[CrossRef](#)]
72. Holzberg, S.; Brosio, P.; Gross, C.; Pogue, G.P. Barley stripe mosaic virus-induced gene silencing in a monocot plant. *Plant J.* **2002**, *30*, 315–327. [[CrossRef](#)]